Synthesis, characterization and catalytic activity of nano-zeolite Y for the alkylation of benzene with isopropanol

Ta Ngoc Don*[,1], Ta Ngoc Hung[1], Pham Thanh Huyen[1], Trinh Xuan Bai[1], Huynh Thi Thanh Huong[2],
Nguyen Thi Linh[3], Le Van Duong[1] & Minh-Hao Pham[4]

[1]School of Chemical Engineering, Hanoi University of Science and Technology, 1 Dai Co Viet, Hanoi 10000, Vietnam
[2]Danang University of Education, 459 Tonducthang, Danang, Vietnam
[3]Hanoi University of Mining and Geology, Dongngac, Tuliem, Hanoi, Vietnam
[4]Department of Chemical Engineering, Centre en catalyse et chimie verte (C3V), Laval University, Quebec, G1V 0A6, Canada
E-mail: don.tangoc@hust.edu.vn

The synthesis and characterization of zeolite NaY nanocrystals (Nano-NaY) from Vietnamese kaolin have been carried out. Nano-NaY has been modified to Nano-USY and used as catalyst for the alkylation of benzene with isopropanol to obtain cumene. Nano-NaY has been succesfully synthesized with surface area of 565 m^2/g (in which external surface area of (102 m^2/g), crystal size of 22 nm, contains both micropores (of 0.81 nm) and mesopores (of 12 nm). The SiO_2/Al_2O_3 ratio increases from 3.87 to 5.52 after the modification of Nano-NaY to Nano-USY.

Recently, zeolite NaY with nanometer particle size (zeolite NaY nanocrystals, nano-NaY) has been synthesized to increase the external surface area and widen the secondary pore system with the pore size dimension within the mesoporous range. Due to the unique properties in the nanometer range, nano-NaY is not only used in conventional applications such as catalysts and adsorbents, but also applied as photo electronic materials, sensors and phamaceuticals[1].

Most recent research studies of nano-NaY synthesis are from clear precursor solution with excess organic templates which are prepared from separated soluble silicon and aluminum sources in alkaline media[2]. TMAOH (tetramethylamonium hydroxide) is usually used as organic templates[2-6]. The crystallization proceeds through several steps: forming clear precursor solutions at room temperature for 72-144 h (Refs. 2-6), hydrothermal crystallization at 60°C and at 95-100°C for 24-48 h (Refs. 4,5) and 24-215 h (Refs. 3-5), correspondingly. NaCl (Ref. 1) or TMABr (tetramethyl-amonium bromide)[2,7] are sometimes added to control the particle sizes. Obtained nano-zeolites have surface area of 407-757 m^2/g (Refs. 3,4) with external surface area of 72-178 m^2/g (Refs. 6), particle sizes of 20-80 nm (Ref. 4,7). The above studies of nano-NaY synthesis were carried out at harsh conditions and high cost.

This paper presents the results of synthesis and characterization of nano-NaY from Vietnamese kaolin by hydrothermal method at atmospheric pressure. The modification of nano-NaY to be used as catalyst for the alkylation of benzene with isopropanol are also discussed.

Experimental Section

Synthesis of nano-NaY

Vietnamese kaolin was treated with solution of HCl 4N with solid/liquid ratio of 2/3 (g/mL) at 90°C for 6 h. The samples were washed until free of Cl⁻ ion, dried at 110°C for 2 h, calcined at 650°C for 3 h at atmospheric pressure. A metastable phase referred to as metakaolin was obtained.

Metakaolin was mixed with sodium hydroxide, sodium chloride, liquid water glass, triethanolamine (noted as TEA) and distilled water with molar ratio of $3.5Na_2O \cdot Al_2O_3 \cdot 7SiO_2 \cdot 70H_2O \cdot 3NaCl \cdot 2TEA$. The obtained mixture was aged at room temperature for 144 h, hydrothermally crystallized at 80°C for 72 h under autogenous pressure.

Nano-NaY products were recovered by filtration, washed repeatedly with distilled water until $pH = 8$, then dried at 110°C and calcined at 550°C.

Commercial NaY zeolite (Strem Chemicals, Inc-France) with micrometer size (noted as micro-NaY) was used as reference.

Modification Nano-NaY to Nano-HY

Nano-NaY synthesized from kaolin and micro-NaY with the same SiO_2/Al_2O_3 ratio of 3.8 was exchanged with 1N NH_4Cl solution with solid/liquid ratio of 1/10 (g/mL) to convert to NH_4Y form. The cation exchange was carried out at room temperature for 5 h. The products were washed to remove Cl^- ion, then dried at 110°C, calcined at 500°C for 5 h. The cation exchanging and calcination were repeated 3 times to convert zeolite from Na^+ form to H^+ form. The final products were noted as nano-HY and micro-HY, correspondingly.

Convert Nano-HY to Nano-USY

In order to increase framework SiO_2/Al_2O_3 ratio to produce more stable catalysts with higher acidity, acetyl acetone solution (ACAC) was used to de-aluminate nano-HY and micro-HY. The de-alumination was carried out in Soxhlet apparatus at 140°C for 6 h. The formation of orange complex between ACAC and aluminum was an indication of the framework de-alumination. The solids were separated and then extracted in Soxhlet at 80°C for 4 h to remove excess ACAC and complex. The products were washed, filtered, dried and calcined under air flow at 500°C for 3 h to obtain nano-USY and micro-USY. Then these samples were pressed and crushed into 20-40 mesh particles for the usage of catalytic testing.

Catalyst characterization

XRD analyses were carried out at room temperature in θ–2θ reflection mode using a SIEMENS D5005 diffractometer. SEM and TEM images were obtained on JSM 5410 LV and JEM 1010. FTIR was performed on Nicolet impact FTIR 410 spectrometer.

Nitrogen adsorption-desorption measurements were carried out at 77 K on a Micromeritics ASAP 2010 instrument to determine the Brunauer–Emmett–Teller (BET) surface area and to estimate the mesopore size distribution using the Barrett–Joyner–Halenda (BJH) calculation procedure. Before each measurement, samples were evacuated overnight at 100°C and < 1 µm Hg. Higher temperatures were not used so that occluded template in the zeolite structure would not decompose or volatize. The total pore volume, V_{total}, was taken from the desorption branch of the isotherm at P/Po = 0.995 assuming complete pore saturation. The volume of the micropores, V_{micro}, was determined by the t-plot method. The volume of the mesopores, V_{meso}, was estimated from the equation: $V_{meso} = V_{total} - V_{micro}$.

The Na contents of samples before and after exchanging with NH_4Cl solution were determined by AAS (on AA6501S- Shimadzu). The acidity of catalysts were determined by TPD-NH_3 on Autochem II 2920. SiO_2/Al_2O_3 ratio were analysed by melting method and EDTA titration.

Catalytic activity test

The catalyst (2 g) was activated at 500°C for 2 h with nitrogen. The benzene alkylation were carried out at atmospheric pressure at 200-280°C for 15-60 min in a continuous flowing fixed-bed reactor with benzene/isopropanol = 4:1 (mol/mol) and a WHSV of 3.0 h^{-1}. The products were analyzed by GC (HP 6890- Agilent) with FID detector and SBB1 column (3 m long).

Results and Discussion

Characterization of Nano-NaY, nano-HY and nano-USY

Chemical analysis

By chemical analysis, SiO_2/Al_2O_3 ratio of nano-NaY and micro-NaY were 3.87 and 3.82, respectively. It seemed that nano-NaY still contained a very small amount of SiO_2 in the structure of phlogopit that was the contaminate of the raw materials.

The conversion of NaY to HY zeolite was carried out by cation exchange. The cation exchange capacities were determined by AAS (as shown in Table 1). SiO_2/Al_2O_3 ratio and mole % of Al_2O_3 dissolved in solution were presented in Table 2.

The cation exchange process was very rapid at the first time and slower at the second and the third time. It meant that the cation exchange firstly proceeded on

Table 1 — Cation exchange capacities of nano-NaY and micro-NaY

No	Samples	Cation exchange capacities of Na^+ to H^+, %		
		After 1st time	After 2nd time	After 3rd time
1	Nano-NaY	91.8	96.9	98.2
2	Micro-NaY	89.2	95.3	96.8

Table 2 — SiO_2/Al_2O_3 ratio and molar % of Al_2O_3 dissolved in solution

No	Samples	SiO_2/Al_2O_3 ratio	Molar % of dissolved Al_2O_3
1	Nano-NaY	3.87	-
2	Nano-HY	4.12	6.5
3	Nano-USY	5.52	34.0
4	Micro-NaY	3.82	-
5	Micro-HY	4.05	6.0
6	Micro-USY	5.25	29.6

the surface of the sample and then to the pore of the sample. Na^+ cations that stayed in the pore were exchanged later and very slowly, because it took time for NH_4^+ ions to move to the pore to exchange with Na^+, and then they were decomposed to NH_3 and H^+ ions at high temperature. The long diffusion pathway of NH_4^+ and Na^+ ions made the cation exchange process slow and incomplete. Nano-NaY with smaller particle sizes and shorter diffusion pathway had better cation exchange capacities than micro-NaY at the same exchange condition.

As shown in Table 2 nano-HY and micro-HY samples had higher SiO_2/Al_2O_3 ratio. It meant that during cation exchange process part of alumina had been dissolved in solution and because nano-NaY had better cation exchange capacity, mole% of Al_2O_3 dissolved in solution was higher than micro-NaY (6.5% compared with 6.0%).

Nano-HY and micro-HY with SiO_2/Al_2O_3 ratio of 4.12 and 4.05 were not suitable to be used as catalyst for alkylation[9] because of low SiO_2/Al_2O_3 ratio. The modification to increase SiO_2/Al_2O_3 ratio will produce more thermal and hydrothermal stable catalysts. ACAC were used to de-aluminate zeolite.

SiO_2/Al_2O_3 ratio of nano-USY and micro-USY increased to 5.52 and 5.25, respectively, it indicated that aluminum were extracted from the framework of zeolite by treating with ACAC. The molar% of dissolved Al_2O_3 from the framework of Nano-USY was higher than that from micro-USY (34% compared to 29%). It could be explained by the smaller particle sizes of nano-USY that make the contact of ACAC and Al^{3+} in tetrahedral of AlO_4^- easier so more alumina was extracted from the framework of zeolite.

XRD pattern

XRD patterns of nano-NaY, micro-NaY, nano HY and micro-HY were shown in Fig. 1.

XRD pattern of micro-NaY (Fig. 1b) represents only one crystalline phase of zeolite NaY with the formula of *1.03*$Na_2O \cdot Al_2O_3 \cdot$ *3.8*$SiO_2 \cdot$ *8*H_2O (PDF 38–0240) with straight baseline, strong and sharp peak and small line width. It proved that micro-NaY zeolite has high crystallinity and large particle sizes.

XRD pattern of nano-NaY (Fig. 1a) showed that beside crystalline phase of NaY zeolite a trace of phlogopit (PDF 02–0053) also appeared which might be due to the contaminant in the raw materials. The intensity of nano-NaY was less than that of micro-NaY (53%) and the line width increased, which indicated that the particles sizes of nano-NaY zeolite
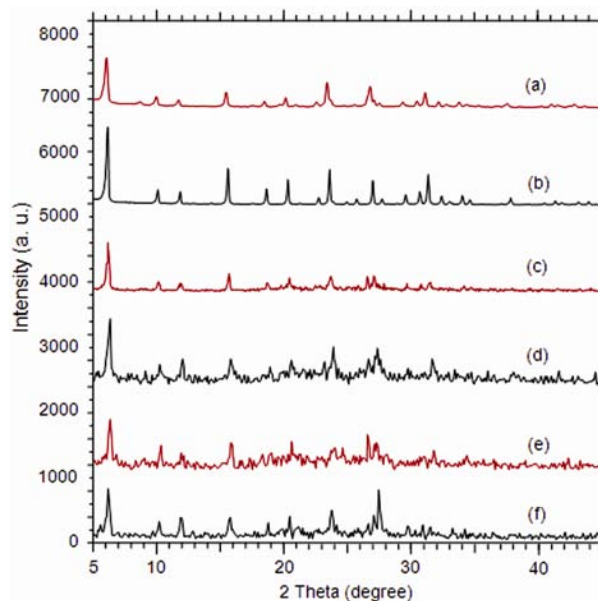

Fig. 1 — XRD patterns of nano-NaY (a), micro-NaY (b), nano-NaY (c), micro-HY (d), and dealuminated nano-USY (e) and micro-USY (f)

were smaller. The crystallite sizes of nano-NaY and micro-NaY calculated by Scherrer's formula[11] were 19 and 400 nm, respectively.

XRD patterns of nano-HY and micro-HY after exchanged 3 times with NH_4Cl were given in Figs. 1c and 1d. It can be seen that the baselines were not smooth and the intensity of the typical diffraction of Y zeolite were lower than that of precursor Na^+ form (compared to Figs 1a and 1b). It meant that during the conversion of Na^+ to H^+, part of zeolite crystals were destroyed. There was no strange phase appeared after exchange process, it proved that the frameworks of zeolite were unchanged.

The intensities of peaks corresponding to Y zeolite on XRD patterns of de-aluminated zeolites (Figs 1e and 1f) were lower than that of their precursors (Figs 1c and 1d), it indicated the partly collapse of zeolite crystals accompanying with the dealumination.

SEM and TEM images

SEM images of nano-NaY and micro-NaY (Fig. 2a and 2b) showed that both samples contained well-formed cubic crystals with diameter of 165 and 620 nm, correspondingly. TEM image (Fig. 2c) indicated that nano-NaY has particle size of 22 nm.

The particle sizes of nano-NaY measured by XRD and TEM are in nano scale of 19 and 22 nm, correspondingly, whereas when measuring by SEM, it is 165 nm. It might be because of the low resolution of SEM method.
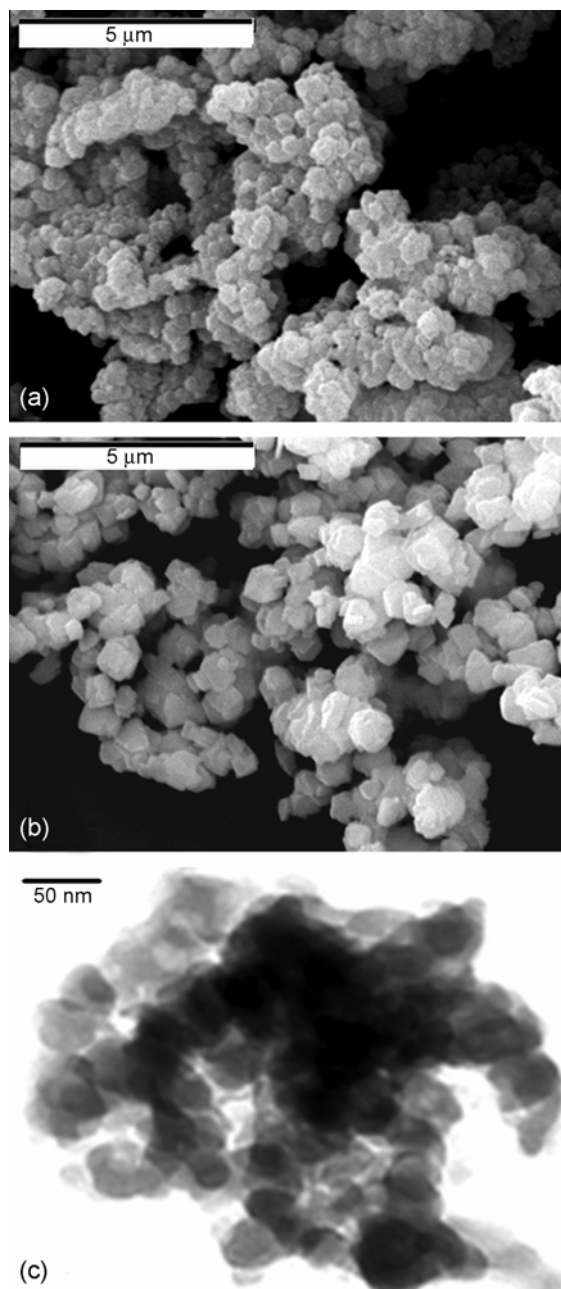
Fig. 2 — SEM images of nano-NaY (a), micro-NaY (b) and TEM image of nano-NaY (c)

FTIR and SiO_2/Al_2O_3 ratio

FTIR spectra of nano-NaY, micro-NaY, nano HY, micro-HY, nano-USY and micro-USYare shown in Fig. 3. All key bands of nano-NaY resemble those exhibited by micro-NaY, the intensities of absorption bands at 570 cm^{-1} which is attributed to the double 6-member-ring of zeolite NaY are similar. It indicated that the crystallinity of these two zeolites is not very different (according to XRD the crystallinity of nano-NaY is 95% and that of micro-NaY is 100%).
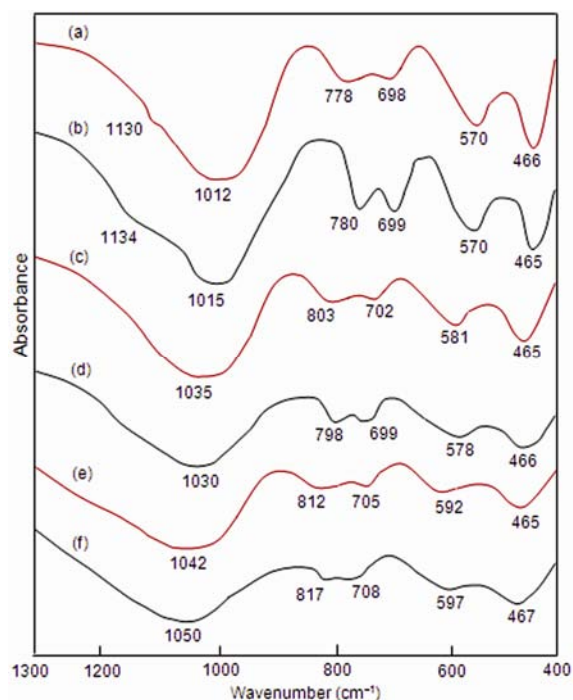

Fig. 3 — FT-IR spectra of nano-NaY (a) and micro-NaY (b), nano-HY (c), micro-HY (d), nano-USY (e) and micro-USY (f)

However, the peaks at 778 and 698 cm^{-1} (in nano-NaY sample) which are assigned to external linkage symmetrical stretching and internal tetrahedra symmetrical stretching, respectively[3] has weaker intensity of that at 780 and 699 cm^{-1} (in micro-NaY). It might be explained by the smaller particle sizes of nano-NaY than micro-NaY.

FT-IR spectra of nano-HY and micro-HY were shown in Figs 3c and 3d. All the vibration peaks (except peak at 465-466 cm^{-1} which correspond the vibration of amorphous aluminosilicate) shifted to the higher wave number and had lower intensity than that of un-exchanged sample (compared to Figs 3a and 3b). It indicated that the ratio of SiO_2/Al_2O_3 of H^+ samples were higher than that of Na^+ samples.

Moreover, peaks corresponding to zeolite crystallinity at 578-581 cm^{-1} of H^+ zeolites had lower intensity than that of Na^+ zeolites. It was also consistent with the results obtained from XRD patterns (Fig. 1) and chemical analysis (Table 2) that part of aluminum content was dissolved in solution during the cation exchange process that leaded to higher SiO_2/Al_2O_3 ratio and lower crystallinity due to the collapse of partly zeolite framework.

The partly collapse of zeolite crystals accompanying with the dealumination was proved with IR spectra (Figs 3e and 3f) in which the vibration

peaks moved to higher wavelength and had lower intensity than un-dealuminated samples.

Specific surface area and pore distribution (BET model)

N_2 adsorption/desorption isotherms at 77 K of nano-NaY (a) and micro-NaY are shown in Fig. 4. The isotherm of micro-NaY is belong to type I (defined by IUPAC) which is the characteristic of microporous materials, whereas, the loop started at $P/P_o \approx 0.55$ can be observed in the isotherm of nano-NaY, which belongs to type IV[8] because of the condensation of nitrogen in mesopores of the materials. These mesopores could be formed between the nanometer crystals.

Both samples have high adsorbed volume at $P/P_o \sim$ 0, it proves that they all have high surface area (565 and 579 m^2/g, respectively – Table 3).

Pore distribution of nano-NaY and micro-NaY are shown in Figs 4c and 4d. The average pore sizes of both micro-NaY and nano-NaY are 0.81 nm. However, pore distribution in ~ 12 nm region can be observed in nano-NaY, it might be the secondary porous system formed between the nanometer crystals and causes the loop in the isotherm that can be seen in Figs 4a and 4b.
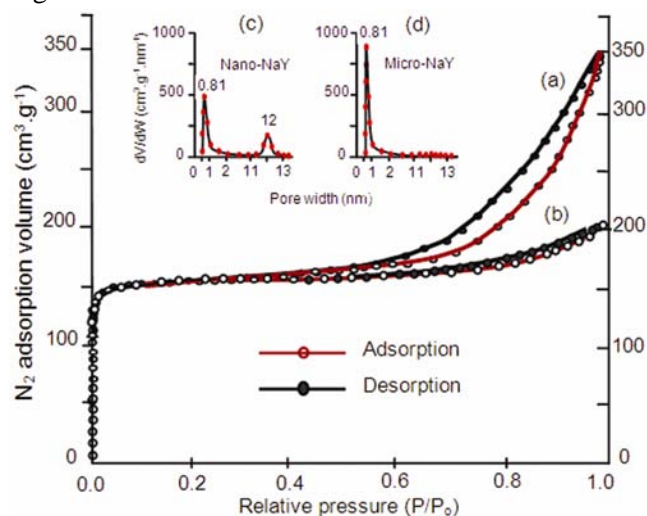

Fig. 4 — N_2 adsorption-desorption isotherms of nano-NaY (a) and micro-NaY (b) and Pore distribution of nano-NaY (c) and micro-NaY (d)

The BET surface areas of nano-NaY was lower than that of micro-NaY, but the external surface of nano-NaY is larger (102 m^2/g compared to 37 m^2/g). The increasing of the external surface is due to the reducing in crystal sizes (Table 3).

Specific surface area, pore distribution and pore volume of nano-USY and micro-USY were presented in Table 4. It can be seen that the sample treatment did not change the pore distribution but significantly reduced the specific surface area, total pore volume and micropore volume compared to the original sample (nano-NaY and micro-NaY). These were due to the reduction of crystallinity after the treatment (322 and 320 m^2/g in Table 4 compared with 565 và 579 m^2/g in Table 3, respectively).

The BET surface area, pore distribution and volume of nano-USY and micro-USY were presented in Table 4.

The acidity of catalyst

The acidities of catalysts, determined by TPD-NH_3, were shown in Fig. 5 and Table 5.

Table 4 — BET surface area, pore distribution and pore volume of nano-USY and micro-USY

Sample	BET surface area ($m^2 g^{-1}$)	Pore distribution (nm)	Total pore volume ($cm^3 g^{-1}$)	Micropore volume ($cm^3 g^{-1}$)
Nano-USY	322	0.81; 12.0	0.187	0.119
Micro-USY	320	0.81	0.188	0.107
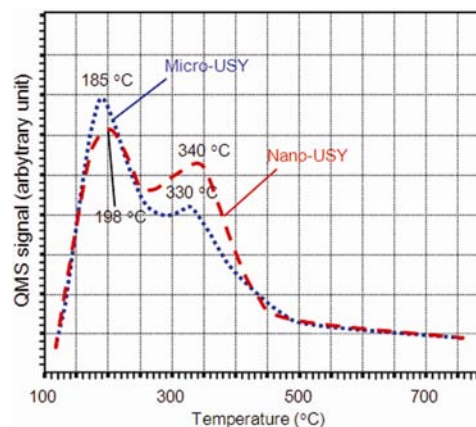
Fig. 5 — TPD-NH_3 profiles of nano-USY and micro-USY

Table 3 — Characteristics of nano-NaY and micro-NaY

Sample	BET surface area ($m^2 g^{-1}$)	External surface area ($m^2 g^{-1}$)	Pore distribution (nm)	Crystal size (nm)			Total pore volume ($cm^3 g^{-1}$)	Micropore volume ($cm^3 g^{-1}$)
				By XRD	By SEM	By TEM		
Nano-NaY	565	102	0.81; 12.0	19	165	22	0.332	0.190
Micro-NaY	579	37	0.81	400	620	-	0.343	0.234

Table 5 — Acidity (mmol/g zeolite) of dealuminated zeolite and its distribution

Samples	Acidity, mmol/g zeolite		Total acidity mmol/g
	Weak acid site	Medium acid site	zeolite
Micro-USY	0.125	0.043	0.168
Nano-USY	0.082	0.071	0.153

Figure 5 showed that both nano-USY and micro-USY contained weak and medium acid sites. However, the desorbed NH_3 peaks of nano-USY appeared at 198 and 340°C, which are higher than that of micro-USY (at 185 and 330°C). The number of weak acid sites in micro-USY (0.125 mmol/L) was higher than that in nano-USY (0.082 mmol/L), whereas the number of medium sites in micro-USY is lower (0.043 compared to 0.071 mmol/L). The total acidity of nano-USY is lower than that of micro-USY. It is consistent with results published by Niken *et al*[10], Singh *et al*[11], Suzuki *et al*[12], Wang *et al*[13], Wang and Wang[14].

TPD-NH_3 showed that the higher the SiO_2/Al_2O_3 ratio, the lower the total acidity (smaller NH_3 desorbed peak area) but the higher the acidity strength (NH_3 desorbed at higher temperature). The decrease of total acidity of nano-USY might be due to the hydroxyl number of framework decreasing, because of the relative increasing of the SiO_2/Al_2O_3 ratio[9].

This result also confirmed that the dealumination from the zeolite framework did not generated amorphous aluminum species but only the complex with ACAC. This complex was then separated from the treated zeolite confirmed by the orange solution when washing the zeolite. This can be considered as the main advantage of ACAC compared with other reagent for the dealumination such as HNO_3 và EDTA.

Catalytic activity of nano-USY for benzene alkylation with isopropanol

Comparison of nano-USY and micro-USY catalytic activity

The catalytic activities of nano-USY and micro-USY for benzene alkylation with isopropanol (IPA) were presented in Table 6.

The results indicated that benzene conversion (28.9%) and cumene selectivity (87.5%) on nano-USY were higher than that on micro-USY (26.5 and 77%, respectively). It might be because nano-USY possessed higher external surface area and smaller particle sizes, so more catalytic active site were easily accessible to the reactants. It is in good agreement with those reported in literature[9]. Further more, the

Table 6 — The catalytic results of the catalysts for alkylation benzene with isopropanol

Catalyst	Nano-USY	Micro-USY
Product composition (wt %)		
Aliphatic	0.2	0.2
Benzene	60.7	64.2
Toluene	0.1	0.1
C8-aromatics (ethyl benzene, xylene)	0.2	3.8
Iso-propyl benzene (cumene)	34.2	27.4
n-propyl benzene (*n*-PB)	0.1	2.5
Di isopropyl benzene (DIPB)	4.5	1.8
Benzene conversion (wt %)	28.9	26.5
Cumene selectivity (wt %)	87.5	77.0

Reaction conditions: benzene/IPA (molar ratio) = 4:1, temperature = 220 °C, WHSV = $3h^{-1}$, pressure = 1 atm, time on stream = 45 min.

higher cumene selectivity on nano-USY might be due to the fact that it had secondary mesoporous channels that were not existed on micro-USY.

The main products of the benzene alkylation with IPA were cumene and di isopropyl benzene (DIPB), other by-products were toluene, xylene, ethylbenzene, *n*-propylbenzene (*n*-PB)[15,16]. Brönsted acidic sites on external surface of zeolites were the main active sites in activating larger molecule such as DIPB. Thus, the selectivity of DIPB on nano-USY was higher than that on micro-USY (4.5% compared to 1.8%), whereas the selectivity of C8-aromatic (ethyl benzene, xylene) and *n*-PB were lower (Table 6).

So, the distributions of weak and medium-strength-acidic sites were important factors for alkylation reaction. Nano-USY had better selectivity to cumene due to the fact that their diameters were in nano scale and they possessed secondary mesoporous channel that were not existed on micro-USY.

Influence of reaction temperature

Influence of reaction temperature on the benzene alkylation with IPA on nano-USY was shown in Table 7. The benzene conversion and cumene selectivity got the maximum results at 220°C with benzene conversion of 28.9% and cumene selectivity of 87.5%. The increasing of DIPB and *n*-PB selectivity at high temperature leaded to the decreasing of cumene selectivity.

It seemed that 220°C was the optimal temperature for the benzene alkylation with IPA on nano-USY zeolite at atmospheric pressure.

Influence of reaction time on stream

The influences of time on stream on activation of nano-USY catalyst were presented in Table 8.

Table 7 — Effect of temperature on activity of nano-USY

Temperature (°C)	200	220	240	260	280
Product composition (wt %)					
Aliphatic	0.2	0.2	0.2	0.2	0.2
Benzene	63.4	60.7	61.0	62.8	63.5
Toluene	0.1	0.1	0.1	0.1	0.1
C8-aromatics (ethyl benzene, xylene)	0.1	0.2	0.3	0.4	0.4
Iso-propyl benzene (cumene)	31.1	34.2	33.6	31.2	29.9
n-propyl benzene (n-PB)	0.1	0.1	0.3	0.3	0.3
Di isopropyl benzene (DIPB)	5.0	4.5	4.5	5.0	5.6
Benzene conversion (wt%)	26.5	28.9	28.7	27.0	26.3
Cumene selectivity (wt%)	85.4	87.5	86.6	84.3	82.4

Reaction conditions: benzene/IPA (molar ratio) = 4:1, WHSV = 3h^{-1}, pressure = 1 atm, time on stream = 45 min.

Table 8 — Effect of time on stream on activity of nano-USY

Time on stream (min.)	30	45	60	75	90
Product composition (wt %)					
Aliphatic	0.1	0.2	0.3	0.3	0.4
Benzene	62.6	60.7	68.1	75.6	84.3
Toluene	0.1	0.1	0.1	0.1	-
C8-aromatics (ethyl benzene, xylene)	0.2	0.2	0.2	0.2	0.3
Iso-propyl benzene (cumene)	32.6	34.2	27.3	20.0	11.7
n-propyl benzene (n-PB)	0.1	0.1	-	-	-
Di isopropyl benzene (DIPB)	4.3	4.5	4.0	3.8	3.3
Benzene conversion (wt %)	27.3	28.9	22.6	16.6	10.0
Cumene selectivity (wt%)	87.4	87.5	86.4	79.7	76.5

Reaction conditions: benzene/IPA (molar ratio) = 4:1, WHSV = 3h^{-1}, pressure = 1 atm, temperature = 220°C.

The catalysts deactivated rapidly after 45 minutes. The cumene and DIPB selectivity decreased while other by-product selectivities such as toluene, ethyl benzene, xylene and n-PB stayed the same. It might be due to the coke formation which covered the active sites to deactivate the catalysts. The formation of coke might partly block the pores of the catalysts or narrower both micro- and mesopores of zeolites, so the amount of large molecule such as DIPB decreased[17].

Catalyst stability

Catalyst stability is an important factor for catalysts. In this work, after each run, catalyst was regenerated by heating at high temperature in dry air flow to burn off coke deposited on the surface. Table 9 presented the results obtained after the 1st, 5th and 10th run.

Table 9 — Effect of catalyst stability on activity of Nano-USY

Product composition (wt %)	1st run	5th run	10th run
Aliphatic	0.2	0.2	0.2
Benzene	60.7	61.6	63.6
Toluene	0.1	0.5	0.9
C8-aromatics (ethyl benzene, xylene)	0.2	0.6	1.2
Iso-propyl benzene (cumene)	34.2	32.6	29.7
n-propyl benzene (n-PB)	0.1	0.2	0.2
Di isopropyl benzene (DIPB)	4.5	4.3	4.2
Benzene conversion (wt %)	28.9	28.3	26.6
Cumene selectivity (wt %)	87.5	85.3	82.0

Reaction conditions: benzene/IPA (molar ratio) = 4:1, temperature = 220°C, WHSV = 3h^{-1}, pressure = 1 atm, time on stream = 45 min.

The results showed that benzene conversion and cumene selectivity decreased slightly after 5th and 10th run. After 10 runs, the cumene selectivity was still > 81%. It indicated that coke was easily burned off the catalyst.

The alkylation reactions were carried out under mild condition (at low temperature and atmospheric pressure). The main products were cumene with high selectivity. It proved that nano-USY was a suitable catalyst for benzene alkylation with isopropanol. The results of alkylation reaction on nano-USY were comparable to those on mordenite, MCM-56 and MCM-22 (Ref. 9), AlPO$_4$-5, MAPO-5, ZAPO-5 and MnAPO-5 (Ref. 17), SAPO-5 (Ref. 18), ZSM-5, ITQ-22, SSZ-33 and Beta/Ge[19].

Conclusion

Nano-NaY has been succesfully synthesized from Vietnamese kaolin. The materials has crystallinity of 95%, surface area of 565 m^2/g, external surface area of 102 m^2/g, pore distribution at micropore range of 0.81 nm and mesopore range of 12 nm, crystal size of 22 nm.

Nano-USY has been produced from nano-NaY by cation exchange with NH$_4^+$, followed by calcination and then treated with ACAC. Nano-USY had SiO$_2$/Al$_2$O$_3$ ratio of 5.52, surface area of 322 m^2/g, pore distribution at 0.81 and 12 nm, weak and medium acidic sites with total acidity of 1.53 mmol/g, that is suitable to be used as catalysts for reactions that required medium-strength acidity.

Catalytic activity of nano-USY is tested for benzene alkylation with isopropanol and compared to that of micro-USY. The results show that benzene conversion and cumene selectivity of reaction on

nano-USY were higher than that on micro-USY. The optimal conditions for this reaction at atmospheric pressure, benzene/IPA molar ratio of 4/1 and WHSV of 3 h^{-1} are at 220°C and time on stream of 45 min. nano-USY is found to be stable after 5th run.

Acknowledgements

References

1   Tosheva L & Valtchev V P, *Chem Mater*, 17 (2005) 2494.
2   Brett A H, Huanting W, Joseph M N & Yushan Y, *Micro Meso*, 59 (2003) 13.
3   Tao Y, Kanoh H & Kaneko K, *J Phys Chem*, 107 (2003) 10974.
4   Yi H, Kun W, Dehua D, Dan L, Matthew R H, Anita J H & Huanting W, *Micro Meso Mater,* 127 (2010) 167.
5   Larlus O, Mintova S & Bein T, *Micro Meso Mater*, 96 (2006) 405.
6   Song W, Grassian V H & Larsen S C, *Chem Commun*, 23 (2005) 2951.
7   Morales-Pacheco P, Alvarez F, Bucio l & Domínguez J M, *J Phys Chem*, C 113 (2009) 2247.
8   Michal K & Mietek J, *Chem Mater*, 13 (2001) 3169.
9   Zuowang Z, Wanchun Z, Shubo Z, Mingjun J, Wenxiang Z & Zhenlu W, *J Porous Mater*, 20 (2013) 531.
10   Niken T, Abdul R M & Subhash B, *J Nanopart Res*, 13 (2011) 3177.
11   Singh M, Kamble R & Viswanadham N, *Catal Lett*, 120 (2008) 288.
12   Suzuki K, Aoyagi Y, Katada N, Choi M, Ryoo R & Niwa M, *Catal Today*, 132 (2008) 38.
13   Kunyuan W, Xiangsheng W & Gang L, *Micro Meso Mater*, 94 (2006) 325.
14   Kunyuan W & Xiangsheng W, *Micro Meso Mater*, 112 (2008) 187.
15   Corma A, Forne´s V, Forni L, Ma´rquez F, Martı´nez-Triguero J & Moscotti D, *J Catal*, 179 (1998) 451.
16   Corma A, Martı´nez-Soria V & Schnoeveld E, *J Catal*, 192 (2000) 163.
17   Sridevi U, Narayan C P, Rao B K B, Satyanarayana C V & Rao B S, *Catal Lett*, 79 (2002) 1.
18   Joseph A R K & Vijayraghavan V R, *J Chem Sci*, 116 (2004) 107.
19   Corma A, Francisco J Ls, Martínez C, Sastre G & Valencia S, *J Catal*, 268 (2009) 9.